How to Cite:
Rawat, S., & Ghate, M. (2022). Benzimidazole-Urea derivatives as anti-cancer agents: In-silico study, synthesis and in-vitro evaluation. *International Journal of Health Sciences*, *6*(S5), 5187–5217. https://doi.org/10.53730/ijhs.v6nS5.9764

Benzimidazole-Urea derivatives as anti-cancer agents: In-silico study, synthesis and in-vitro evaluation

Sushama Rawat
Department of Pharmaceutical Chemistry, Institute of Pharmacy, Nirma University, S. G. Highway, Ahmedabad 382481, Gujarat, India
Email: sushamar07@gmail.com

Manjunath Ghate
Department of Pharmaceutical Chemistry, Institute of Pharmacy, Nirma University, S. G. Highway, Ahmedabad 382481, Gujarat, India
Email: manjunath.ghate@nirmauni.ac.in

***Abstract*---**A new series of urea derivatives containing benzimidazole group as potential anticancer agents have been designed and synthesized. The structures of the synthesized compounds were characterized and confirmed by spectroscopic techniques such as ^{1}H NMR, and Mass spectrometry. A new series of urea derivatives containing benzimidazole group were design with an intention to search new antiproliferative lead compound. Drug like properties and bioactivity score for drug targets of designed compounds were calculated by molinspiration tool and obtained result found to obey Lipinski's rule that indicates the compound are orally active molecules. Osiris property explorer was used for the prediction of drug relevant properties and toxicity of synthetic compounds. Pre ADMET server was also used to estimate ADME properties of synthetic compounds, results showed good to notable anticancer activity. So that, these new benzimidazole-urea compounds could serve as potential template to become leads in near future for the discovery and development of new effect orally drugs molecules. Two compounds, SRA13 [1-(2,3-Dimethylphenyl)-3-(1-methyl-1H-benzo[d]imidazol-2-yl)urea] and SRA20[1-(3-Chloro-4-fluorophenyl)-3-(1-methyl-1H-benzo[d]imidazol-2-yl)urea] were exhibited highest drug score and emerged as lead compounds and motivates for further development of more effective and safer compounds.Compound SRA20 showed the most effective activity against the lungs cancer cell lines (IC50 = 1.9µM) and EGFR binding (IC50 =0.93µM) affinity as compared to other members of the series.

International Journal of Health Sciences ISSN 2550-6978 E-ISSN 2550-696X © 2022.
Manuscript submitted: 27 Feb 2022, Manuscript revised: 9 April 2022, Accepted for publication: 18 June 2022

***Keywords*---**Benzimidazole, Urea, Lipinski's rule, OSIRIS property explorer, Pre ADMET, Antiproliferative activity, T.E.S.T tool.

1. Introduction

Cancer affects both the well being and the capital of the person who has it. During the life of a nutrient dense species, cells die and divide to keep building up new tissue. To stay alive, it is important to maintain a careful balance between the two. Damage to the DNA can throw off the balance, leading to growths that don't belong. So, cancer is a word for a malady in which cells that shouldn't be dividing do so without regulation (uncontrolled cell proliferation). Cancer spreads to neighbouring tissues and other areas of the body through the circulating blood and lymph vessels (metastasis) [1-3]. In recent years, many cancer-fighting medications have been developed. Many present treatments are ineffective because they are toxic to typical fast-growing cells, leading to medication resistance. Most available drugs aren't specific [4]. Therefore, effective, less toxic anticancer drugs are needed.

Molecular biology, empirical screening, and rational medication development have found many heterocyclic and fused heterocyclic compounds [5-6]. Nitrogen-containing heterocyclic systems, such as azoles, are vital in the quest for anticancer drugs. Benzimidazole nuclei are important in biological and synthetic medicinal chemistry searches. It has long been known that benzimidazole derivatives have a variety of beneficial properties, including cancer/antitumor/antiproliferative [7–17], inflammatory [11], antifungal, antioxidant [19] and antiviral including anti-HIV [20], antibacterial, and cysticidal [22] activities. Based on earlier scientific journals, the current study project involves design, synthesis, characterisation, in-silico analysis, and in-vitro anticancer activity. (Figure 1).

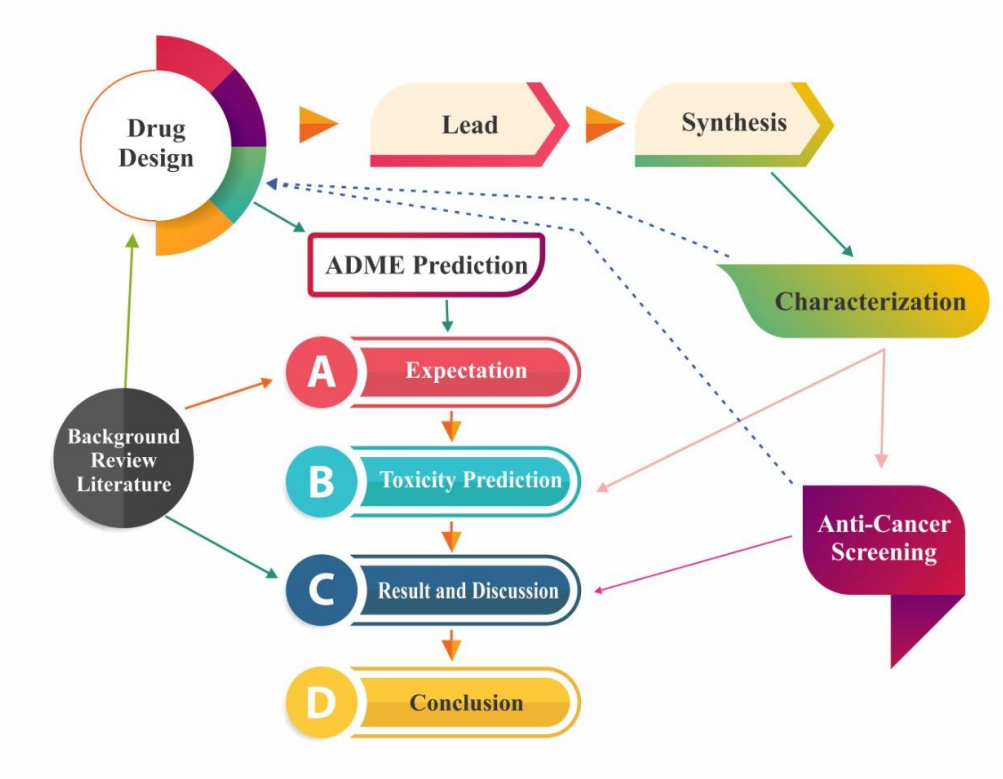

Figure 1. Research Outline for the Discovery of Novel Anti-Cancer agents

Urea and Thio-urea kinds of organic compound that can be used in many different ways. Their compounds have various pharmacological properties, including antibacterial, antidiabetic, analgesic, and anticancer effects[28-34]. Several anticancer drugs with urea and thiourea functional groups, like Tandutinib and Enzalutamide, have reached the clinical phase (Figure 1). In addition, a series of benzimidazole-urea [31]and benzimidazole-thiourea [32] derivatives were synthesized and showed strong antiproliferative activity against a subset of human tumor cells in comparison to gold-standard therapies. Powerful anticancer action was observed in hybrids of urea and benzimidazole, and several derivatives, including Glasdegib [33], are now available as drugs. (Figure 2).

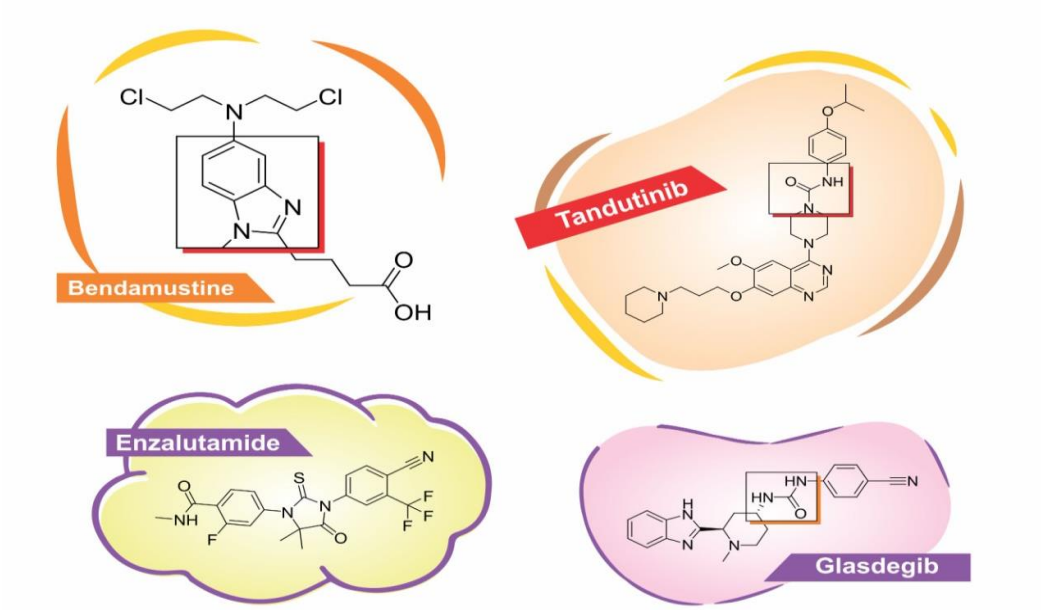

Figure 2: Rationally design and template for synthetic Scheme from marketed anticancer drug

2. Material and Methods

2.1. General information

Melting points were measured using an uncorrected liquid paraffin bath in open capillary tubes. Toluene, ethyl acetate, and formic acid (5:3:2, v/v/v) and benzene, acetone (9:1, v/v) were utilized as solvents while TLC plates (silica gel G) were used to track the reactions' development. After exposing the skin to iodine vapors or ultraviolet light, the spots may be pinpointed. PerkinElmer Spectrum Version 10.4.00 FT-IR spectrophotometer was used to record the spectra (USA). Spectra were obtained using a Varian-400 MHz NMR spectrometer and a CDCl3 or DMSO-d6 solvent at room temperature for the 1H NMR spectra. Both the CDCl3 and DMSO-d6 solvent peaks were utilized as internal standards (7.26 [D] and 77.2 [C] ppm and 2.50 [D] and 39.7 [C] ppm, respectively). The chemical shifts are assigned using data from routine nuclear magnetic resonance (NMR) tests (1H and 13C). TLC tests were conducted on silica F254 using UV light at 254 nm for detection. By means of collision-induced dissociation on a Bruker APEX-4 (7-Tesla) instrument, high resolution mass spectra (HRMS) were acquired (in positive or negative mode) using the electrospray ion trap (ESI) technique. Silica Gel 60 was used for the chromatographic column (230 mesh). Our chemistry supplies came from Sigma-Aldrich Chemical Co.

2.2. Synthesis Compounds (SRA11-SRA20) by Scheme 1.

We synthesized Benzimidazole-Urea derivatives [SRA11-SRA20] as follows. *O*-Phenylene diamine [1] reacts with cyanogen bromide in methanol at room temperature and followed by ammonium hydroxide workout gives 2-amino benzimidazole [2] with 88% yield.

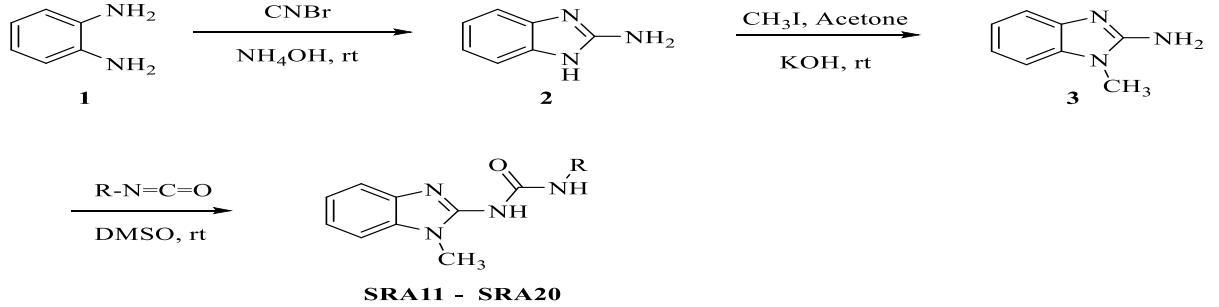

Compound	R	Compound	R
SRA11	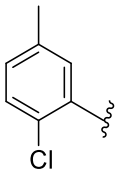	SRA16	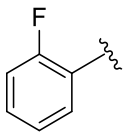
SRA12	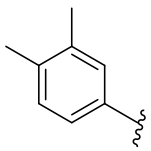	SRA17	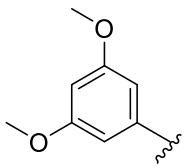
SRA13	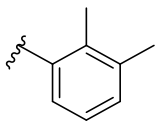	SRA18	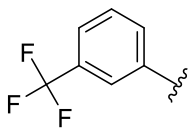
SRA14	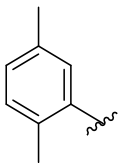	SRA19	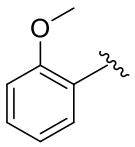
SRA15	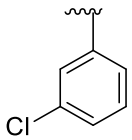	SRA20	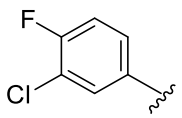

Scheme 1: Synthesis of Benzimidazole –urea derivatives(SRA11-SR20)

Synthesis of 2-amino benzimidazole (2):
To a mixture of methanol and water (1:1) cyanogen bromide (1.5 mol)and o-phenylene diamine(1) (1.00 mol) and was stirred at room temperature for 24 h. After, the methanol was removed obtained oily residue was cooled using ice and treated with ammonia. Continuous stirring for 1 hour, solids precipitated were collected and recrystallized from ethanol/water. Yield 88 %, m.p. 234 °C; ^{1}H NMR (400 MHz, $CDCl_3$): δ 7.2 (dd, 2H, *J*= 5.8), 6.9 (dd, 2H, *J*= 5.8), 5.4 (s, 2H), 4.8 (s, 1H). We synthesized N-methylbenzimidazole derivatives [SRA11-SRA20] as follows : *O*-Phenylene diamine [1] reacts with cyanogen bromide in methanol at room temperature and followed by ammonium hydroxide workout gives 2-amino benzimidazole [2] with 88% yield. 2-aminobenzimidazole on N-methylation with methyl iodide in acetone medium in presence of basic condition yielded 2-amino-1-methyl benzimidazole [3]. In the last step compound 3 reacts with various substituted phenyl isocyanate in DMSO medium under room temperature gives target compounds [SRA11-A20]

Preparation of 1-methyl-1H-benzo[d]imidazol-2-amine (3):
2-Aminobenzimidazole (2) (1.00 equiv) in acetone mixed with KOH (5.00 equiv), to the above slurry methyl iodide (1.10 equiv) was added slowly at stirred at room temperature for one hour. Reaction mixture filtered through sintered funnel and filtrate concentrated and purified using column chromatography to afford compound **3** as brown solid. Yield 79%: ^{1}H NMR (300 MHz, DMSO-d_6) δ 3.47 (s, 3H), 6.34 (br s, 2H), 6.82-6.92 (m, 2H), 7.06-7.09 (m, 2H).

General procedure for the preparation of compounds SRA-11 to SRA-20:
1-Methyl-1H-benzo[d]imidazol-2-amine (3)(1.00 mmol) was mixed to dimethyl sulfoxide under nitrogen atmosphere, and then the corresponding (sub)phenyl isocyante (1.05 mmol) was added at room temperature and continued stirring for 30 minutes. After the completion of reaction [TLC] reaction mixture mixed to water and extracted with dichloromethane. Organic layer washed with brine and separated the layers, organic layer concentrated to get crude compounds. Crude compounds purified using recrystallization in ethanol to afford final compounds (**SRA-11 to SRA-20**).
1-(2-Chloro-5-methylphenyl)-3-(1-methyl-1H-benzo[d]imidazol-2-yl)urea (SRA-12): Yield: 71%, ^{1}H NMR (400 MHz, DMSO-d_6):δ 11.31 (1H, br s), 9.57 (1H, br s), 7.62 (1H, s), 7.39 (1H, d, *J* = 7.7 Hz), 7.22 – 7.19 (2H, m), 7.14 (2H, m), 7.01 (1H, d, *J* = 7.6 Hz), 3.47 (3H, s), 2.38 (3H, s), 2.24 (3H, s).
1-(2,3-Dimethylphenyl)-3-(1-methyl-1H-benzo[d]imidazol-2-yl)urea (SRA-13): Yield: 82%, ^{1}H NMR (400 MHz, DMSO-d_6):δ 11.32 (1H, br s), 9.57 (1H, br s), 7.29 (1H, m), 7.22 – 7.19 (6H, m), 3.47 (3H, s), 2.32 (3H, s); 2.17 (3H, s).
1-(2,5-Dimethylphenyl)-3-(1-methyl-1H-benzo[d]imidazol-2-yl)urea (SRA-14): Yield: 81%, ^{1}H NMR (400 MHz, DMSO-d_6):δ 11.31 (1H, br s), 9.57 (1H, br s), 7.31 (1H, s), 7.21 – 7.19 (3H, m), 7.14 (2H, d, *J* = 7.6 Hz), 7.01 (1H, d, *J* = 7.6 Hz), 3.47 (3H, s), 2.39 (3H, s); 2.28 (3H, s).
1-(3-Chlorophenyl)-3-(1-methyl-1H-benzo[d]imidazol-2-yl)urea (SRA-15): Yield: 79%, ^{1}H NMR (400 MHz, DMSO-d_6):δ 11.28 (1H, br s), 9.61 (1H, br s), 7.98 (1H, s), 7.40 (1H, d, *J* = 7.7 Hz), 7.37 (2H, m), 7.28 (1H, d, *J* = 7.7 Hz), 7.21 – 7.19 (2H, m), 7.12 (1H, d, *J* = 7.6 Hz),3.47 (3H, s).

1-(2-Fluorophenyl)-3-(1-methyl-1H-benzo[d]imidazol-2-yl)urea (SRA-16): Yield: 64%, ^{1}H NMR (400 MHz, DMSO-d_6):δ 11.31 (1H, br s), 9.66 (1H, br s), 7.91 (1H, s), 7.73 (1H, t, J = 7.9 Hz), 7.28 – 7.21 (5H, m), 7.16 (1H, m),3.47 (3H, s).
1-(3,5-Dimethoxyphenyl)-3-(1-methyl-1H-benzo[d]imidazol-2-yl)urea (SRA-17): Yield: 78%, ^{1}H NMR (400 MHz, DMSO-d_6):δ 11.28 (1H, br s), 9.59 (1H, br s), 7.26 (2H, d, J = 7.7 Hz), 7.22 – 7.19 (2H, m), 7.01 (2H, s),7.01 (1H, s)3.74 (6H, s),3.43 (3H, s).
1-(1-Methyl-1H-benzo[d]imidazol-2-yl)-3-(3-(trifluoromethyl)phenyl)urea (SRA-18): Yield: 56%, ^{1}H NMR (400 MHz, DMSO-d_6):δ 11.30 (1H, br s), 9.48 (1H, br s), 8.24 (1H, s), 7.76 (1H, d, J = 7.9 Hz), 7.41 – 7.39 (2H, m), 7.22 – 7.19 (2H, m), 7.14 (2H, d, J = 7.7 Hz),3.51 (3H, s).
1-(2-Methoxyphenyl)-3-(1-methyl-1H-benzo[d]imidazol-2-yl)urea (SRA-19): Yield: 66%, ^{1}H NMR (400 MHz, DMSO-d_6):δ 11.42 (1H, br s), 9.46 (1H, br s), 8.24 (1H, s), 7.91 (1H, d, J = 7.9 Hz), 7.33 (1H, m), 7.29 (1H, m), 7.26 (1H, d, J = 7.9 Hz), 7.22 – 7.19 (2H, m), 7.14 (2H, d, J = 7.7 Hz), 3.79 (3H, s),3.51 (3H, s).
1-(3-Chloro-4-fluorophenyl)-3-(1-methyl-1H-benzo[d]imidazol-2-yl)urea (SRA-20): Yield: 63%, ^{1}H NMR (400 MHz, DMSO-d_6):δ 11.39 (1H, br s), 9.42 (1H, br s), 7.87 (1H, s), 7.38 (1H, d, J = 7.9 Hz), 7.32 (1H, d, J = 7.9 Hz), 7.22 – 7.19 (2H, m), 7.14 (2H, d, J = 7.7 Hz)3.51 (3H, s).

2.3 Study of in-silico assessment

2.3.1. Drug likeness and Lipinski's rule

Rule of molecular characteristics for predicting drug pharmacokinetics (ADME; Absorption, distribution, metabolism, and excretion) was developed in 1997 by Christopher A. Lipinski. The alteration of molecular structure frequently results in medications with a greater molecular weight, more rings, a greater number of rotatable bonds, and a greater lipophilicity. The rule is significant for drug development in which a pharmacologically active lead molecule is incrementally improved for greater activity, selectivity, and drug-like characteristics. The rule asserts that poor absorption or penetration is more likely if a ligand molecule violates the Lipinski rule of 5, that is, if it contains more than five hydrogen bond donors, a molecular weight more than 500, a log P greater than 5, and a total of nitrogen and oxygen greater than 10 [35]. A complicated balance of multiple chemical attributes and structural characteristics determines whether a specific molecule resembles established medications. This includes bioavailability, transport properties, affinity to proteins, reactivity, toxicity, and metabolic stability [36-38].

2.3.2. Drug-likeness Prediction

This screening approach was performed to assess the drug-likeness of suggested ligands as it affects the behavior of molecules in live organisms, including bioavailability, transport characteristics, affinity to proteins, reactivity, toxicity, and metabolic stability [35-36]. Pre ADMET provides a module for predicting drug-likeness based on Lipinski's criteria. In addition, a number of drug-like criteria, such as the Ghose filter [39], CMC [40], WDI [41], and MDDR DB [42], can be used to identify drug-like properties. Ghose filter establishes drug-likeness limitations as follows: computed log P is between -0.4 and 5.6, molecular weight is between 160 and 480, molar refractivity is between 40 and

130, and the number of total atoms is between 20 and 70 [38]. The developed filter differentiates between drug-like and non-drug-like chemical substances.

2.3.3. Molinspiration and Prediction of Drug likeness

The molecular structures and smiles notations of synthesized substances were derived using Chem. Bio draw Ultra (11.0 versions) program (Table 1). Smiles notations of benzimidazole derivatives were then fed into Molinspiration (2018.02 version) and drug likeness tool to calculate numerous molecular properties (Tables 3 & 4) and to predict bioactivity score for drug targets, such as enzymes and nuclear receptors, kinase inhibitors, GPCR ligands, and ion channel modulators (Table 5). To evaluate the drug-likeness of the synthesized compounds, molecular properties such as partition coefficient (Log P), topological polar surface area (TPSA), hydrogen bond donors and acceptors, rotatable bonds, number of atoms, molecular weight, and violations of Lipinski's rule of five were calculated and displayed in Table 3. percent Ab was also determined using the following formula: percent Ab = 109 - [0.345 x TPSA] (Table 3). These properties are calculated according to Lipinski's rule of five, which states that any compound considered to be a drug must have a partition coefficient of less than 5, a polar surface area within 1402, a H bond acceptor of less than 10, a H bond donor of less than 5, and a molecular weight within 500 dalton [43-48].

Table 1: Compound names and their smiles of Benzimidazole Urea derivatives (SRA11-20).

Compound	Smiles Notation
SRA11	Cc3ccc(Cl)c(NC(=O)Nc2nc1ccccc1n2C)c3
SRA12	Cc3ccc(NC(=O)Nc2nc1ccccc1n2C)c(C)c3
SRA13	Cc3ccc(NC(=O)Nc2nc1ccccc1n2C)cc3C
SRA14	Cc3ccc(C)c(NC(=O)Nc2nc1ccccc1n2C)c3
SRA15	Cn3c(NC(=O)Nc1cccc(Cl)c1)nc2ccccc23
SRA16	Cn3c(NC(=O)Nc1ccccc1F)nc2ccccc23
SRA17	COc3cc(NC(=O)Nc2nc1ccccc1n2C)cc(OC)c3
SRA18	Cn3c(NC(=O)Nc1cccc(C(F)(F)F)c1)nc2ccccc23
SRA19	COc1ccccc1NC(=O)Nc3nc2ccccc2n3C
SRA20	Cn3c(NC(=O)Nc1ccc(F)c(Cl)c1)nc2ccccc23

Molinspiration is used to calculate the subsequent molecular characteristics. LogP: The total of fragment-based contributions and correction factors. Topological Polar Surface Area (TPSA): The total of fragment contributions. O- and N-centered polar pieces are taken into account. It has been demonstrated that TPSA is an excellent descriptor for describing drug absorption, including intestinal absorption, bioavailability, Caco-2 permeability, and blood-brain barrier penetrance. Molecular volume is the total of fragment contributions to the true 3D volume for a training set of over 12,000 molecules, the vast majority of which are drug-like. Five Property Precepts: The rule specifies that the majority of drug-like compounds have logP = 5, molecular weight =500, and the number of hydrogen bond acceptors = 10 and the number of hydrogen bond donors = 5. Molecules breaching many of these principles may have bioavailability issues. The rule is known as the "Rule of 5" because to the fact that the boundary values are 5, 500,

2*5, and 5. n-rotb stands for the number of rotatable bonds. A rotatable bond is any non-ring bond attached to a nonterminal heavy (non-hydrogen) atom and a measure of molecular flexibility. Due to their high rotational energy barrier, C-N amide bonds are disregarded [36, 49-53]. Similarity to pharmaceuticals may be characterized as a complex balance of multiple chemical attributes and structural characteristics that determine whether a molecule is comparable to recognized medications. These properties, specifically hydrophobicity, electronic distribution, hydrogen bonding characteristics, molecule size, flexibility, and the presence of various pharmacophoric features, influence the behavior of a molecule in a living organism, including bioavailability, transport properties, affinity to proteins, reactivity, toxicity, and metabolic stability, among others [35-36, 51-53].

2.3.4. Osiris Property Explorer and Drug Relevant Properties Prediction

Property Explorer is a free tool that can be used to predict the physicochemical and toxicological properties of molecules. These properties need to be optimized when making compounds that are used in healthcare. It was created by T. Sander and implemented by Actelion Pharmaceutical Ltd. as an integral part of the compound licensing system in the drug development division. It is now the de facto standard for predicting physicochemical properties and indicating toxicity risk. For anticipating drug-relevant characteristics of a chemical compound, just sketch its structure; property explorer will begin calculating properties as soon as a valid chemical structure has been drawn. Prediction findings are assigned a numerical value and color coding [54- 55].

Properties having a high risk of adverse consequences, such as mutagenicity or poor intestinal absorption, are displayed in red. In contrast, green represents stimulant behavior. Charges should be equalized, and atom valances should not be exceeded. Nitro-groups, for example, must be shown with a positive charge on nitrogen and a negative charge on one of the oxygen atoms, with a single bond joining these two atoms. The OSIRIS property explorer drug-relevant properties and toxicity risk evaluation are shown in Tables 6 and 7. These are the important features and toxicity risk of the medication. Compounds having greater weights are less likely to be absorbed and, hence, to ever reach the site of action. lopP forecast: Low hydrophilicity and hence high logP values result in inefficient absorption or penetration. It has been demonstrated that for chemicals to have a decent chance of being adequately absorbed, their logP value cannot exceed 5.0. Aqueous Solubility: The aqueous solubility of a substance has a substantial impact on its absorption and distribution properties. It demonstrates that the computed logS value of more than 80 percent of commercially available medications is more than -4. Topological polar surface area: If the contributions among all polar atoms exposed on a molecule's surface add up to an area more than 80 or 100 2, the possibility of the molecule easily passing through membranes is diminished. There are a number of methods that evaluate the drug-likeness of a chemical based in part on topological descriptors, fingerprints of MDL structure keys, or other features such as cLogP and molecular weights. The drug score integrates drug similarity, cLogP, logS, molecular weight, and toxicity concerns into a single number that may be used to evaluate a compound's overall ability to qualify as a medicine [56-62].

2.3.5. Toxicity Assessment

As long as the structure being drawn represents a real chemical entity, the toxicity risk predictor will immediately begin searching for any possible toxicity issues. Toxicity risk alerts show that the structure that was drawn could be harmful based on the risk category that was given. But risk alerts are not meant to be a 100% accurate way to predict how dangerous something is. The results of predictions are looked at and given colors. Red shows properties that aren't good or that have a high risk of side effects, like mutagenicity or poor absorption in the gut. Instead, drug-conform behavior is shown by the color green. To make sure that no harmful substances are used in the next steps of preclinical studies, the toxicity risk assessment must be done. The risks of mutagenic, tumorigenic, irritant, and reproductive toxicity were measured using a set of pre-calculated structural fragments that were made based on how compounds were categorized in the Registry of Toxic Effects of Chemical Substances (RTECS) database. With a color code, the risks of toxicity can be estimated. The effects of the molecule that are not wanted (toxic risks) are shown in red, while the effects that are wanted are shown in green [58–62, 63–64].

2.3.6. Pre ADMET

Unfortunately, ADME/Toxicity issues accounted for the failure of over half of the choices. The majority of pharmaceutical firms have established a series of in-vitro ADME/Toxicity screens with the intention of rejecting compounds in the discovery process that are prone to failure further down the road. Even though early stage in-vitro ADME testing makes it less likely that a drug will fail during development, it still takes a lot of time and resources. Pre-ADMET is made up of the following four main parts. Molecular descriptor calculation: Properties like lipophilicity (logP), molecular weight, polar surface area, and water solubility are closely related to ADME/toxicity properties. How a drug will be liked: Pre ADMET has a module that predicts how similar a drug is to Lipinski's and Lead-like. ADME Prediction: The Caco2 cell model and the MDCK (Madin Darby canine kidney) cell model have been suggested as reliable in-vitro models for predicting how drugs will be absorbed when taken by mouth. Also, the in-silico HIA (human intestinal absorption) model and the skin permeability model can predict and find potential drugs for oral delivery and transdermal delivery. Blood-brain barrier (BBB) penetration can disclose details about a therapeutic drug's effect on the central nervous system (CNS) and its effectiveness [38, 41, 64, 65].

2.3.7. Acute toxicity prediction

Toxicity prediction is becoming more and more important in the early stages of drug discovery, since it is the reason why 30% of active compounds fail. The mutagenicity of the Ames test and the T.E.S.T. tool (Version 4.2.1), which is a program from the US Environmental Protection Agency, were used to figure out how dangerous something was. Ames test: Dr. Ames came up with the Ames test, which is a simple way to find out if a compound can cause mutations. Several strains of the bacterium Salmonella typhimurium are used. These strains have mutations in genes that make histidine, so they need histidine to grow. Ames TA100 (+S9); An Ames test done in a lab showed that the TA100 strain (Metabolic activation by rat liver homogenate). Ames TA100 (-S9); An in-vitro test of Ames showed that the TA100 strain (No metabolic activation). Ames TA1535 (+S9); Ames tests done in a lab showed that the TA1535 strain (Metabolic activation by

rat liver homogenate). Ames TA1535 (-S9); An Ames test done in a lab showed that the TA1535 strain (No metabolic activation) [64-66]. Tool of the T.E.S.T program: This is a software program made by the US Environmental Protection Agency to figure out how dangerous a compound is in the short term. QSAR/QSPR (Quantitative structure– activity relationship/Quantitative structure–property relationship) representation was being used in tool for the estimation of toxicity of synthetic as well as natural compounds. The tool uses different types of descriptors that are based on the structural features of compounds [69–71].

3. Result and Discussion

The purity of compounds was checked by single-spot TLC using Toluene: Ethyl acetate: Formic acid (5:4:1) and Benzene: Acetone (9:1) solvent systems and spots located under iodine vapors/UV light. The structures of the synthesized compounds were established on the basis of modern analytical techniques; ^{1}H-NMR, Mass spectral data and elemental analysis. The title compounds were synthesized in three steps, as outlined in Scheme 1. o-phenylene diamine and Cyanogen bromide were added to methanol and water and mixed for 24 hours at room temperature. The oily residue was chilled with ice and then treated with ammonia after the methanol was extracted. After the mixture of ethanol and water was stirred continuously for an hour, the solids that had precipitated out were collected and recrystallized from ethanol/water mixture. The purity of the prepared compound is confirmed by recrystallization,its melting point, chromatographic technique, and spectroscopy. The newly synthesized compounds (SRA11-20) were characterized by MS, 1H NMR,spectral data. These data, detailed in the experimental part, are consistent with the suggested structures. The HRMS of the synthesized compounds are in good agreement with the calculated values.The diversity of the proposed compounds in Scheme 1 is evident from the urea functional group substitution on the phenyl ring including activating and deactivating groups data and deactivating groups. These structure variations can help investigating the structure–activity relationship.

3.1. In-silico data prediction

3.1.1. Prediction of Physicochemical properties

Depending on Lipinski's rules of five, the Molinspiration server was used to look at the molecular descriptors and drug-likeness of compounds. Pharmaceutical chemists often use Lipinski's rule of five to figure out how well a possible future lead or drug molecule will work when taken orally. The rule says that most molecules that look like drugs have a logP of less than 5, a molecular weight of less than 500 daltons, and fewer than 10 hydrogen bond acceptors and fewer than 5 hydrogen bond donors. Molecules that break more than a few of these rules might have trouble being absorbed by the body. Physical and chemical parameters are very important in creating and increasing the bioactivity of a chemical [35,36].

Molinspiration was used to find parameters like Log P, TPSA, and drug likeness. LogP (octanol/water partition coefficient) is a measure of how hydrophobic a molecule is. It is used in QSAR studies and rational drug design. Hydrophobicity

affects how drugs are absorbed, their bioavailability, how they interact with hydrophobic receptors, how molecules are broken down, and how toxic they are. It is found by adding up the contributions of each fragment and the correction factors being used predict how easily a molecule can pass through the cell membrane. This method was developed by Molinspiration. Topological polar surface area (TPSA) is a really beneficial parameter for predicting how drugs move through cells. The polar surface area of a molecule is the sum of the surfaces of its polar atoms, which are usually oxygen, nitrogen, and hydrogen atoms that are attached. The following formula was also used to figure out the absorption percentage (percent Ab): percent Ab = 109 - [0:345 x TPSA] (Table 3) [38-42].

Lipinski's rule of five was used to test the molecular descriptions of synthetic compounds. It's interesting that all of the ligands have molecular weights between 330 and 450 (500). Drug molecules with a low molecular weight (less than 500) are easy to move. Unlike heavy molecules, light molecules are spread out and taken in. Molecular weight is an important part of how therapeutic drugs work, and if it goes up, it changes how the drug works. The amount of hydrogen bond donors (NH and OH) in the tested samples was less than 5, and the number of hydrogen bond acceptors (O and N atoms) was also less than 10, with the exception of compounds SRA15, SRA16,SRA17,SRA20 and SRA19. The logP value and the TPSA value are two significant properties that can be used to predict how well a drug will work when taken by mouth. Topological polar surface area (TPSA) has been determined to be within the range. As polar fragments, O- and N-oriented ones were looked at. TPSA has been shown to be a very good way to describe drug absorption, including intestinal absorption, bioavailability, Caco-2 permeability, and BBB penetration. The compounds were found to have the highest level of lipophilicity. This means that they are good at dissolving in lipids, which will help the drug interact with membranes. TPSA was found by adding up the surface areas of the oxygen, nitrogen, and hydrogen atoms that are attached to them. So, the TPSA is strongly connected to a compound's ability to form hydrogen bonds. Except for compounds SRA15, SRA16, SRA17, and SRA19, all of the compounds in this study had a TPSA value between 87.92 and 139.45, which shows that they are well absorbed when taken orally. Compounds with less than 10 rotatable bonds and a TPSA of less than 140 are more likely to be well absorbed by the body. As the quantity of bonds that can be rotated goes up, the substance becomes more adaptable and better able to fit into a binding pocket. All compounds are interesting because they have 7-8 bonds that can be rotated and are adaptable within the Lipinski threshold [43–46].

Tables 3 and 4 show the calculated molecular properties of drugs (SRA11-20). The compounds didn't break Lipinski's rule of five or the Ghose filter, but only compounds SRA15, SRA16,SRA17,SRA19 and SRA20. were found to have no violations (one violation detected). The compounds had 0–1 violations, so it is likely that they can be taken by mouth. The hydrophobicity or lipophilicity of a molecule is shown by the Log P or partition coefficient. The Log P values of the substances were noticed to be less than 5, and they don't break Lipinski's rule of five or the Ghose filter. This suggests that the compounds can pass through cell membranes easily. Compounds were found to have a molecular weight of less than 500. This means that these molecules should be easier to move, spread, and absorb than large molecules. Lipinski's rule of five says that the number of

hydrogen bond donors (NH and OH) in the man-made compounds should be less than 5. The TPSA of the compound was found to be between 87.92 and 139.45, which is less than 160. Absorption percentages measured using TPSA ranged from 51.38 to 78.67, indicating high oral absorption (Table 2). For all compounds SRA12(134.53), where the molar refractivity falls inside the Ghose filter, the range was determined to be 93.94-107.09. (Table 3).

Table 2: Lipinski's rule of five predicted the physicochemical characteristics of compounds. (SRA11-20)

Compd.	% Abs	miLog P o/w	TPSA (A^0)	n atoms	MW	n-ON	n-OHNH	n-violation	n-rotb	MV
RO5		<5			<500	<10	<5	≤1		
SRA11	78.57	0.73	87.95	22	314	6	2	0	8	271.10
SRA12	78.67	3.39	87.92	31	294	7	1	0	8	274.18
SRA13	74.68	-0.35	102.18	27	294	9	2	0	7	274.18
SRA14	62.15	0.31	138.78	31	294	10	3	0	7	274.18
SRA15	56.70	-1.45	151.57	28	300	11	3	1	7	257.62
SRA16	51.48	-0.31	166.34	30	284	12	4	1	7	245.99
SRA17	53.66	-1.25	160.28	30	326	12	3	1	7	292.15
SRA18	65.09	-1.13	127.42	26	334	10	2	0	7	272.30
SRA19	54.64	-1.37	139.45	28	296	11	3	1	7	266.61
SRA20	59.62	-1.05	157.62	29	318	11	3	1	7	259.53

%Abs: Percentage of absorption, TPSA: Topological polar surface area, n atoms: Number of atoms, n-rotb: Number of rotatable bonds, MW: Molecular weight, MV: Molecular volume, miLogP: Logarithm of partition coefficient between n-octanol and water, n-OHNH: Number of hydrogen bond donors, n-ON: Number of hydrogen bond acceptors, n violations: Number of “Rule-of-five ” violation, RO5: Rule of five.

Table 3: Ghose filter predicted drug likeness properties of compounds (SRA11-SRA20).

Compd.	logP	Molar Refractivity	Number of atoms	Polar Surface Area	Color Indication
Ghose filter	-0.4-5.6	40-130	20-70	<140	Green
SRA11	1.883	93.94	24	66.62	Green
SRA12	3.431	134.53	32	66.62	Pink
SRA13	0.606	104.71	27	69.86	Green

SRA14	1.506	116.21	31	100.76	Green
SRA15	1.227	98.73	28	100.76	Green
SRA16	-0.576	108.15	30	103.7	Green
SRA17	0.806	107.09	30	108.41	Green
SRA18	1.038	91.77	25	91.34	Green
SRA19	0.722	99.79	28	96.07	Green
SRA20	1.235	103.31	29	100.76	Green

3.2.2. Score of biological efficiency

In addition, the compounds' bioactivity was evaluated by computing their activity scores as GPCR (G-protein coupled receptor) ligands, ion channel modulators, kinase inhibitors, and nuclear receptor ligands [31, 47, 48]. The compounds had good affinity for GPCR ligands, and compounds SRA13,SRA16,SRA20 had excellent affinity for GPCR ligands. Compounds also exhibited remarkable enzyme inhibitor activity, and compounds SRA14,SRA16,SRA18,SRA19 found to have amazing enzyme inhibitor activity. Compounds 4k and 4l were good at stopping proteases from working, and compounds 4f were better at stopping kinases from working. The results show that compound SRA16is better than Nuclear receptor ligand and compound 4k are better ligands for GPCR ligand > Protease inhibitor > Kinase inhibitor > Ion channel modulator > Nuclear receptor ligand. Predictions based on in-silico data show that compound SRA13 is also a superior ligand for enzyme inhibition and GPCR (Enzyme inhibitor > GPCR > Kinase inhibitor > Protease inhibitor > Ion channel modulator > Nuclear receptor ligand). If a molecule's bioactivity score is more than 0, it's likely to have a lot of biological activities. If the score is between -0.50 and 0, it's likely to be only moderately active, and if it's less than -0.50, it's likely to be inactive [47–50]. Based on the bioactivity scores, the most promising compounds, like SRA13,SRA20, were found. These compounds are thought to work in more than three ways (Table 4).

Table 4: Predicted bioactivity score of compounds (SRA11-20).

Compd.	3D Structure	GPCR ligand	Ion channel modulator	Kinase inhibitor	Nuclear receptor ligand	Protease inhibitor	Enzyme inhibitor
SRA11	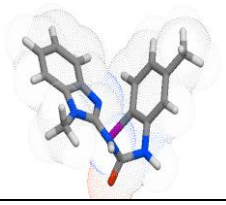	0.15	-0.14	-0.15	-0.52	0.05	0.12
SRA12	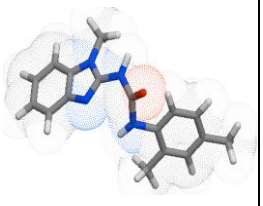	0.13	-0.05	-0.05	-0.15	0.03	0.18

SRA13	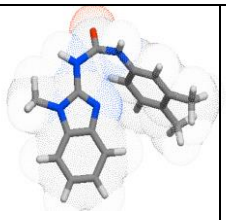	0.25	-0.11	-0.03	-0.54	0.08	0.10
SRA14	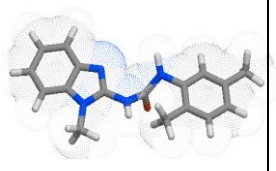	0.05	-0.28	-0.11	-0.55	-0.03	0.21
SRA15	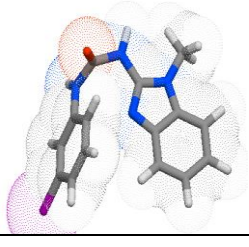	-0.01	-0.41	-0.33	-0.74	-0.05	0.10
SRA16	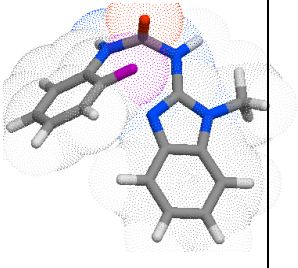	0.28	-0.12	0.26	-0.94	-0.00	0.48
SRA17	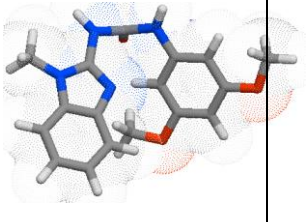	0.07	-0.47	-0.20	-1.10	-0.30	0.14
SRA18	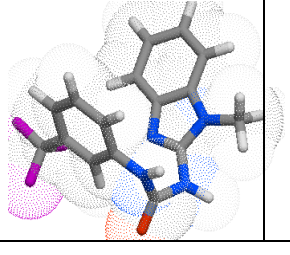	0.08	-0.28	-0.12	-0.65	0.01	0.24

SRA19	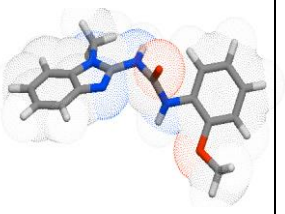	0.13	-0.39	-0.00	-0.87	0.12	0.31
SRA20	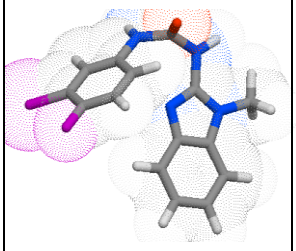	0.27	-0.10	-0.27	-0.55	0.22	0.15

GPCR= G-protein coupled receptor, >0- active, -5.0-0.0- moderately active, < -5.0- inactive.

3.2.3 Osiris property explorer

To evaluate compounds for their pharmacokinetic properties, including toxicity, solubility, drug-likeness, and drug score (www.organicchemistry. org/prog/peo/), we utilized Osiris property explorer. The findings of virtual screening are scored and given a green, red, or yellow color code based on things like their effect on mutagenicity, the reproductive system, irritation, and the ability to cause cancer. Properties that are red show that there is a high risk of unwanted effects, while properties that are green show that the drug behaves as expected, works well with other drugs, and is safe in-vivo [54, 55]. This program makes predictions based on how similar the functional groups of the compound being studied are to the functional groups of compounds in its database that have been studied in-vitro and in-vivo a lot. The results showed that all compounds with a green color, except for SRA11 (which had a yellow color for its irritant effect), were safe and shouldn't cause cancer, mutagenesis, skin irritation, or problems with the reproductive system. Table 5 shows the results of the toxic effects risks, drug likeness score, and drug score for each compound.

Table 5: Osiris property explorer toxicity and drug-relevant features prediction of compounds (SRA11-20).

Compound	Toxicity				Drug-relevant properties			
	Tumorigenic	Reproductive effect	Irritant effect	Mutagenicity	cLogP	Solubility	Drug-likeness	Drug Score
SRA11	Green	Green	Yellowish red	Green	1.31	-1.47	5.41	0.55
SRA12	Green	Green	Green	Green	2.85	-4.73	1.18	0.56
SRA13	Green	Green	Green	Green	-0.85	-0.53	6.87	0.91
SRA14	Green	Green	Green	Green	0.24	-2.69	0.54	0.67
SRA15	Green	Red	Green	Green	-1.58	-2.04	2.85	0.86
SRA16	Green	Green	Green	Green	0.03	-5.47	-0.7	0.4
SRA17	Green	Red	Green	Green	-1.41	-2.36	5.13	0.85
SRA18	Green	Green	Green	Green	-2.05	-2.13	-0.87	0.56
SRA19	Green	Green	Green	Green	-3.14	-1.97	5.96	0.86
SRA20	Green	Green	Green	Green	-1.05	-1.97	5.96	0.86

No risk or low risk is indicated by a green color, moderate risk by yellow, and high toxicity risk by red.

3.2.4. ADME and the prediction of toxicity

To determine a compound's ADME (Absorption, Distribution, Metabolism, and Excretion) and toxicity profile, the PreADMET database was used. Because oral dosage is so common, intestinal absorption of the medicine must be a primary consideration for optimal therapeutic efficacy. Some crucial properties highlighted by Lipinski's rule of five were indeed the general prerequisite for medication absorption. Optimal absorption and bioavailability were demonstrated by the compounds, and the rule of five was satisfied, as indicated by the compounds' LogP, TPSA, MW, nON, nOHNH, nviolation, nrotb, and MV data [63–65]. A number of in-vitro approaches have been developed for reliable and precise prediction of intestinal absorption. The Caco-2 cell system is the most widely used in vitro model of intestinal permeability [51]. In the apical membrane of cells, P-glycoprotein (P-gp) activity may reduce the drug's bioavailability [76].

3.2.5. Prediction of ADME/T Properties

Pre ADMET server tallied the results of the HIA (Human Intestinal Absorption), BBB (Blood-Brain Barrier) penetration, Caco-2 cell permeability, and Ames test [37, 39, 63]. Pre ADMET server data indicated that compounds 4a, 4b, and 4d had high human intestinal absorption (HIA) scores. Higher HIA values suggest enhanced intestine absorption after oral administration of the drug. The presence of mutagenicity in a chemical was determined by its performance on the AMES toxicity test. The AMES toxicity test resulted in a negative for the tested molecule, indicating that the majority of the ligands examined were safe [77,78]. Results from the toxicity prediction research show that the proposed chemical was expected to be carcinogenic in rats and to be carcinogenic in mice (Table 6).

Table 6: Toxicity prediction by Pre ADMET server of compounds (SRA11-20).

Compd.	Toxicity prediction	Name of Test	Values of Test
SRA11	Ames test	Ames TA100 (+S9)	-
		Ames TA100 (-S9)	-
		Ames TA1535 (+S9)	-
		Ames TA1535 (-S9)	+
	Carcinogenicity	Carcinogenicity (Mouse)	-
		Carcinogenicity (Rat)	+
SRA12	Ames test	Ames TA100 (+S9)	-
		Ames TA100 (-S9)	-
		Ames TA1535 (+S9)	-
		Ames TA1535 (-S9)	-
	Carcinogenicity	Carcinogenicity (Mouse)	-
		Carcinogenicity (Rat)	+
SRA13	Ames test	Ames TA100 (+S9)	-
		Ames TA100 (-S9)	-
		Ames TA1535 (+S9)	-
		Ames TA1535 (-S9)	-
	Carcinogenicity	Carcinogenicity (Mouse)	-
		Carcinogenicity (Rat)	+

SRA14	Ames test	Ames TA100 (+S9)	+
		Ames TA100 (-S9)	+
		Ames TA1535 (+S9)	-
		Ames TA1535 (-S9)	-
	Carcinogenicity	Carcinogenicity (Mouse)	-
		Carcinogenicity (Rat)	+
SRA15	Ames test	Ames TA100 (+S9)	-
		Ames TA100 (-S9)	+
		Ames TA1535 (+S9)	-
		Ames TA1535 (-S9)	+
	Carcinogenicity	Carcinogenicity (Mouse)	-
		Carcinogenicity (Rat)	+
SRA16	Ames test	Ames TA100 (+S9)	-
		Ames TA100 (-S9)	+
		Ames TA1535 (+S9)	-
		Ames TA1535 (-S9)	-
	Carcinogenicity	Carcinogenicity (Mouse)	-
		Carcinogenicity (Rat)	+
SRA17	Ames test	Ames TA100 (+S9)	-
		Ames TA100 (-S9)	+
		Ames TA1535 (+S9)	-
		Ames TA1535 (-S9)	+
	Carcinogenicity	Carcinogenicity (Mouse)	-
		Carcinogenicity (Rat)	+
SRA18	Ames test	Ames TA100 (+S9)	+
		Ames TA100 (-S9)	+
		Ames TA1535 (+S9)	-
		Ames TA1535 (-S9)	+
	Carcinogenicity	Carcinogenicity (Mouse)	-
		Carcinogenicity (Rat)	+
SRA19	Ames test	Ames TA100 (+S9)	+
		Ames TA100 (-S9)	+
		Ames TA1535 (+S9)	-
		Ames TA1535 (-S9)	+
	Carcinogenicity	Carcinogenicity (Mouse)	-
		Carcinogenicity (Rat)	+
SRA20	Ames test	Ames TA100 (+S9)	-
		Ames TA100 (-S9)	-
		Ames TA1535 (+S9)	-
		Ames TA1535 (-S9)	-
	Carcinogenicity	Carcinogenicity (Mouse)	-
		Carcinogenicity (Rat)	+

-: Negative; +: Positive

It has been shown that these limitations are strongly linked to how well a drug is absorbed by the human gut, how well it passes through the Caco-2 monolayers, and how well it gets through the blood-brain barrier. It was thought that the compound with the least polar chemical structure would be able to cross the

BBB, and the results are shown in Table 8. Based on a method published by Ertl [36], Molecular Polar Surface Area (MPSA) is defined as the summation of fragment-based contributions. O- and N-centered polar fragments are measured and calculated by the surface areas used by the oxygen, nitrogen, and active hydrogen atoms that are attached to them. Molecules' transport properties, like being absorbed by the intestines or getting through the blood-brain barrier, are controlled by their molecular volume (MV). Because of this, Molecular volume is used in QSAR studies to design the properties of molecules and how they work in living things. Molinspiration's method for figuring out the size of a molecule is based on the contributions of groups. The number of bonds that can be rotated (nrotb) is a simple topological factor that shows how flexible a molecule is.

Table 7: ADME/T prediction by Pre ADMET tool compounds (SRA11-20).

Compd.	Toxicity prediction	Name of Test	Values of Test
SRA11	Absorption	HIA, % (Human intestinal absorption)	92.215603
		Caco-2 cell permeability in nm/sec (*In-vitro*)	15.7825
		MDCK cell permeability in nm/sec (*In-vitro*)	215.717
		Skin permeability (logKp) in cm/hour (*In-vitro*)	-4.11061
	Bioavailability	Buffer solubility in mg/ml	367.222
		Pure water solubility in mg/ml	1247.44
	Distribution	Plasma protein binding % (*In-vitro*)	47.279628
		Blood-brain barrier penetration (*In-vivo*) (C. brain/C. blood)	0.0493072
SRA12	Absorption	HIA, % (Human intestinal absorption)	95.342099
		Caco-2 cell permeability in nm/sec (*In-vitro*)	27.4034
		MDCK cell permeability in nm/sec (*In-vitro*)	37.0983
		Skin permeability (logKp) in cm/hour (*In-vitro*)	-2.86615
	Bioavailability	Buffer solubility in mg/ml	4.12198
		Pure water solubility in mg/ml	0.389741
	Distribution	Plasma protein binding % (*In-vitro*)	95.889629
		Blood-brain barrier penetration (*In-vivo*) (C. brain/C. blood)	0.207344
SRA13	Absorption	HIA, % (Human intestinal absorption)	88.872345
		Caco-2 cell permeability in nm/sec (*In-vitro*)	7.42263

		MDCK cell permeability in nm/sec (*In-vitro*)	2.63357
		Skin permeability (logKp) in cm/hour (*In-vitro*)	-4.98237
	Bioavailability	Buffer solubility in mg/ml	1267.96
		Pure water solubility in mg/ml	1661.14
	Distribution	Plasma protein binding % (*In-vitro*)	28.649417
		Blood-brain barrier penetration (*In-vivo*) (C. brain/C. blood)	0.0584475
SRA14	Absorption	HIA, % (Human intestinal absorption)	91.308684
		Caco-2 cell permeability in nm/sec (*In-vitro*)	1.13618
		MDCK cell permeability in nm/sec (*In-vitro*)	2.52908
		Skin permeability (logKp) in cm/hour (*In-vitro*)	-4.95527
	Bioavailability	Buffer solubility in mg/ml	3.02145
		Pure water solubility in mg/ml	0.346366
	Distribution	Plasma protein binding % (*In-vitro*)	80.038452
		Blood-brain barrier penetration (*In-vivo*) (C. brain/C. blood)	0.0465817
SRA15	Absorption	HIA, % (Human intestinal absorption)	75.207209
		Caco-2 cell permeability in nm/sec (*In-vitro*)	1.70306
		MDCK cell permeability in nm/sec (*In-vitro*)	0.833755
		Skin permeability (logKp) in cm/hour (*In-vitro*)	-5.12146
	Bioavailability	Buffer solubility in mg/ml	185.214
		Pure water solubility in mg/ml	154.972
	Distribution	Plasma protein binding % (*In-vitro*)	54.013105
		Blood-brain barrier penetration (*In-vivo*) (C. brain/C. blood)	0.0420603
SRA16	Absorption	HIA, % (Human intestinal absorption)	83.700104
		Caco-2 cell permeability in nm/sec (*In-vitro*)	1.7489
		MDCK cell permeability in nm/sec (*In-vitro*)	0.687794
		Skin permeability (logKp) in cm/hour (*In-vitro*)	-5.1046

	Bioavailability	Buffer solubility in mg/ml	28.2703
		Pure water solubility in mg/ml	4.12212
	Distribution	Plasma protein binding % (*In-vitro*)	60.886301
		Blood-brain barrier penetration (*In-vivo*) (C. brain/C. blood)	0.0549292
SRA17	Absorption	HIA, % (Human intestinal absorption)	73.189010
		Caco-2 cell permeability in nm/sec (*In-vitro*)	0.943094
		MDCK cell permeability in nm/sec (*In-vitro*)	0.457272
		Skin permeability (logKp) in cm/hour (*In-vitro*)	-5.22165
	Bioavailability	Buffer solubility in mg/ml	10.4568
		Pure water solubility in mg/ml	41.8636
	Distribution	Plasma protein binding % (*In-vitro*)	43.962351
		Blood-brain barrier penetration (*In-vivo*) (C. brain/C. blood)	0.0358059
SRA18	Absorption	HIA, % (Human intestinal absorption)	85.778193
		Caco-2 cell permeability in nm/sec (*In-vitro*)	0.502463
		MDCK cell permeability in nm/sec (*In-vitro*)	2.52258
		Skin permeability (logKp) in cm/hour (*In-vitro*)	-5.0398
	Bioavailability	Buffer solubility in mg/ml	163.365
		Pure water solubility in mg/ml	328.207
	Distribution	Plasma protein binding % (*In-vitro*)	60.687062
		Blood-brain barrier penetration (*In-vivo*) (C. brain/C. blood)	0.0421355
SRA19	Absorption	HIA, % (Human intestinal absorption)	75.297321
		Caco-2 cell permeability in nm/sec (*In-vitro*)	2.83561
		MDCK cell permeability in nm/sec (*In-vitro*)	0.581086
		Skin permeability (logKp) in cm/hour (*In-vitro*)	-5.1312
	Bioavailability	Buffer solubility in mg/ml	435.553
		Pure water solubility in mg/ml	63.5098
	Distribution	Plasma protein binding % (*In-vitro*)	38.872860
		Blood-brain	0.0627287

		barrier penetration (*In-vivo*) (C. brain/C. blood)	
SRA20	Absorption	HIA, % (Human intestinal absorption)	76.683939
		Caco-2 cell permeability in nm/sec (*In-vitro*)	2.3402
		MDCK cell permeability in nm/sec (*In-vitro*)	1.91347
		Skin permeability (logKp) in cm/hour (*In-vitro*)	-5.0762
	Bioavailability	Buffer solubility in mg/ml	346.266
		Pure water solubility in mg/ml	98.2177
	Distribution	Plasma protein binding % (*In-vitro*)	57.895070
		Blood-brain barrier penetration (*In-vivo*) (C. brain/C. blood)	0.0395919

BBB indicates compounds can cross blood brain barrier, HIA indicates compounds can absorb through intestine; Caco-2 indicates compounds can cross Caco-2 cell.

3.2.6 Metabolism prediction

By leaving the specificity of fingerprint identification at its default and choosing all models, the Pre ADMET server was able to guess the first phase of the compound's metabolism. The most essential factor is cytochrome P450 (CYP450), which is part of the isozymes group and helps break down drugs, essential fats, steroids, bile acids, carcinogens, and other things. Some of the different types of cytochrome P450 could be stopped from working by several of the compounds that were tested. Cytochrome P450 enzymes are essential for how drugs are broken down in the body. Cytochrome P450 enzymes are a group of heme proteins that are involved in the metabolism of many pharmacologically active compounds. They can cause unwanted side effects and drug interactions [66, 77]. In-silico data show that all of the designed compounds, except for compound SRA19, are substrates for CYP 450 3A4 (non substrate). All compounds except compound SRA11are found to be non-substrates for CYP 450 2D6 and non-inhibitors for CYP 450 2D6. However, compound SRA18 is found to be inhibitors of CYP 450 2C19, CYP 450 2C9, as well as CYP 450 3A4 and substrates for CYP 450 3A4 (Table 8).

3.2.7. Prediction of Drug likeness and Violation for Synthetic Compounds

There are a number of drug-like rules, such as Lipinski's rule, the Ghose filter, the Lead-like rule, CMC, WDI, and MDDR. Based on these different rules, the Pre ADMET server has a drug-likeness prediction module. But Lipinski's rule, which is also known as the "rule of five," is a well-known way to figure out how similar newly designed molecules are to drugs. The Lead-like rule is another well-known rule. It is based on a quantitative study of the chemical structures of

18 pairs of lead and drugs. Ghose filter says that a substance can't be a drug if its measured log P is between -0.4 and 5.6, its molecular weight is between 160 and 480, its molar refractivity is between 40 and 130, and it has between 20 and 70 atoms in total [39]. Rules have been made

Table 8: Cytochrome P450 enzymes and P-glycoprotein inhibition of compounds (SRA11-20).

Compd.	CYP 450 2C19 Inhibition	CYP 450 2C9 Inhibition	CYP 450 2D6 Inhibition	CYP 450 2D6 Substrate	CYP 450 3A4 Inhibition	CYP 450 3A4 Substrate	P-gp inhibitor
SRA11	Non Inhibitor	Non Inhibitor	Non Inhibitor	Substrate	Non Inhibitor	Substrate	Non Inhibitor
SRA12	Non Inhibitor	Non Inhibitor	Non Inhibitor	Non Substrate	Non Inhibitor	Weakly Substrate	Non Inhibitor
SRA13	Non Inhibitor	Non Inhibitor	Non Inhibitor	Substrate	Non Inhibitor	Substrate	Non Inhibitor
SRA14	Inhibitor	nhibitor	Non Inhibitor	Non Substrate	Inhibitor	Substrate	Non Inhibitor
SRA15	Non Inhibitor	Inhibitor	Non Inhibitor	Non Substrate	Non Inhibitor	Weakly Substrate	Non Inhibitor
SRA16	Non Inhibitor	Inhibitor	Non Inhibitor	Non Substrate	Inhibitor	Substrate	Non Inhibitor
SRA17	Non Inhibitor	Inhibitor	Non Inhibitor	Non Substrate	Inhibitor	Substrate	Non Inhibitor
SRA18	Inhibitor	Inhibitor	Non Inhibitor	Non Substrate	Inhibitor	Substrate	Non Inhibitor
SRA19	Non Inhibitor	Inhibitor	Non Inhibitor	Non Substrate	Non Inhibitor	Non Substrate	Non Inhibitor
SRA20	Non Inhibitor	Inhibitor	Non Inhibitor	Non Substrate	Non Inhibitor	Substrate	Non Inhibitor

CYP 450; Cytochrome P450 enzyme, P-gp = P-glycoprotein.

that tell the difference between chemical molecules that look like drugs and those that don't. All of the compounds were found to be like drugs and to fit the MDDR-like rule and the rule of five. Except for compounds SRA17 and SRA19, all of the designed compounds also meet the CMC-like rule. Table 9 shows the results of compounds that were made with different rules.

Table 9: Prediction of Drug likeness/Violation by different rules for compounds (SRA11-20)

Compd.	CMC like Rule		Lead like Rule		MDDR like Rule		Rule of Five		WDI like Rule	
	Rule	Violation	Rule	Violation	Rule	Violation	Rule	Violation	Rule	Violation
SRA11	Qualified	0	Suitable	0	Drug like	0	Suitable	0	Out of 90% cut off	1
SRA1	Qualifie	0	Violate	2	Drug	0	Suitabl	0	Out of 90% cut	2

2	d		d		ike		e		off	
SRA13	Qualified	0	Violated	2	Drug like	0	Suitable	0	Out of 90% cut off	1
SRA14	Qualified	0	Violated	1	Drug like	0	Suitable	0	Out of 90% cut off	0
SRA15	Qualified	0	Violated	2	Drug like	0	Suitable	0	Out of 90% cut off	1
SRA16	Qualified	0	Violated	2	Drug like	0	Suitable	0	Out of 90% cut off	2
SRA17	Not Qualified	1	Violated	2	Drug like	0	Suitable	0	Out of 90% cut off	2
SRA18	Qualified	0	Violated	1	Drug like	0	Suitable	0	Out of 90% cut off	1
SRA19	Not Qualified	1	Violated	2	Drug like	0	Suitable	0	Out of 90% cut off	1
SRA20	Qualified	0	Violated	2	Drug like	0	Suitable	0	Out of 90% cut off	1

3.3. Pharmacological evaluation

3.3.1 *In vitro* EGFR phosphorylation assays

Taking Geftinib as reference compounds, the synthesized compounds (**SRA11-20**) were
evaluated for the EGFR kinase assay. The results suggested that compound **SRA20** (IC50 = 0.93μM), having 3-Chloro-4-fluorophenyl group. The rest of the compounds showed inhibitory activity in the range of 2.1 to 52.5 μM (Table 10).

Table 10. Inhibitory results of substituted Benzimidazole-2-Urea derivatives against two human cancer cell lines and *in vitro* EGFR kinase assay

Compound	EGFR	HepG2 (Liver)	A549 (Lung)
SRA11	2.1	14.7	2.4
SRA12	21.73	28.4	7.4
SRA13	52.5	37.4	74.7
SRA14	2.6	11.9	9.5
SRA15	ND	34.2	ND
SRA16	6.8	57.32	38.5
SRA17	10.4	46.3	>100
SRA18	37.5	>100	68.4
SRA19	>100	>100	12.6
SRA20	0.93	7.5	1.9
5-FU	-	5.0	1.10
Gefitinib		0.010	

3.3.2 In Vitro Cytotoxicity

Pharmacological evaluation of compounds in vitro were determined using MTT assay method against two cancer cell lines HepG2 (liver) and A549 (lung) showed high anti-tumor activities.The IC50 values were reported in Table 10. Regarding the activity against liver cancer cell lines (HepG2), compound SRA20 (3-Chloro-4-fluorophenyl) was the most active one with IC50 value of 7.5μM, whereas antitumor activity of other compounds are in order of **SRA14> SRA11> SRA12> SRA15> SRA13 >SRA17>SRA 16** with IC50 value range (11.9-57.3μM).

Some of the compounds also showed potent activity against Non-small lung cancer (A549). Among them compound with **SRA20** was the most potent one (IC50 = 1.9 μM), whereas antitumor activity of other compounds are in order of **SRA11>SRA12>SRA 14>SRA 19>SRA 16>SRA18>SRA17** with IC50 value range (2.4-38.5 μM).

The anti-cancer studies on the synthesized compounds from Scheme revealed the structure activity relationship that the nature of substituent on the phenyl substituent attached to the NH of urea group influences the activity. The results from the Table 12 of compounds SRA18, SRA19, SRA20 showed moderate to good cytotoxic activity against A549 (lung cancer cell lines). It is worth pointing out that most significant inhibition shown by compound(SRA20) against A549 cancer cell line with IC50 = 1.9μM. The increase in activity was mainly attributed to the Chloro-fluorophenyl at ortho position of NH of urea group.

Conclusion

In conclusion, we have successfully synthesized a set of 10 new compounds (SRA11-SRA20) that all contain benzimidazole,urea moiety. Synthetic spectra were characterized using, ^{1}H Nuclear Magnetic Resonance, mass spectrometry, and elemental analysis. Each compound was tested for its anticancer properties using an in vitro EGFR kinase assay and two different human cancer cell lines. The results of the screening showed that SRA20 compounds inhibited the growth of cancerous cell lines by a considerable prevalence. Lipinski's rule of five were used to estimate the oral absorption, molecular descriptors, drug-like qualities , bioactivity of compounds and the findings show that the compounds had good oral bioavailability. OSIRIS property explorer anticipated drug relevant properties, and results show that compounds earn a decent drug score, with compounds SRA11, SRA13, and SRA20 receiving great drug likeness and scoring particularly highly.

High lipophilicity, which indicates strong lipid solubility and facilitates drug interaction with membranes, was observed for the synthesized compounds. Compound SRA20 is a potent inhibitor of CYP 450 2C19, CYP 450 3A4, and CYP 2C9, while the other chemicals are all substrates for CYP 450 3A4 with the exception of SRA19. When compared to the other compounds, SRA20 showed the highest drug score and bioactivity score and displayed the best drug-relevant characteristics, ADME, and lack of toxicity. Further study is being conducted to learn more about the SAR and QSAR of SRA13 and SRA20, the two most active compounds in the series.

Conflict of Interest

The authors declare no conflict of interest, financial or otherwise.

Ethical approval: The conducted research is not related to either human or animal use.

Data availability statement: All data are included in this published article.

References

1. Satoh M, Cherian MG (1994) Modulation of resistance to anticancer drugs by inhibition of metallothionein synthesis. Imura Cancer Res 54: 5255.
2. Zhang K, Mack T, Kim PW (1998) Inhibitors of Multidrug Resistance to Antitumor Agents. Int J Oncol 12: 971.
3. Verweij J, Dejonge MJA (2000) Achievements and future of chemotherapy. Eur J Cancer 36: 1479.
4. Volm M (1998) Multidrug resistance and its reversal. Anticancer Res 18: 2905.
5. Vita VT, Hellman S, Rosenberg SA (1992) Cancer principle practical oncology. 4th ed. Philadelphia, J.B. Lippincott, Co., USA.
6. Hartwell LH, Kashan MB (1994) Cell cycle control and cancer. Science 266: 1821.
7. Li Y, Tan C, Gao C, Zhang C, Luan X, Chen X, Liu H, Chen Y, Jiang Y (2011) Discovery of benzimidazole derivatives as novel multi-target EGFR, VEGFR-2 and PDGFR kinase inhibitors. Bioorg Med Chem 19: 4529.
8. Demirayak S, Kayagil I, Yurttas L (2011) Microwave supported synthesis of some novel 1,3-diarylpyrazino[1,2-a]benzimidazole derivatives and investigation of their anticancer activities. Eur J Med Chem 46: 411.
9. Husain A, Rashid M, Siddiqui AA, Mishra R (2013) Benzimidazole clubbed with triazolo-thiadiazoles and triazolo-thiadiazines: New anticancer agents. Eur J Med Chem 62: 785-798.
10. Husain A, Rashid M, Mishra R, Praveen S, Shin DS, Kumar D (2012) Benzimidazole bearing oxadiazole and triazolo-thiadiazoles nucleus: Design and synthesis as anticancer agents. Bioorg Med Chem Lett 22: 5438-5444.
11. Sondhi SM, Rani R, Singh J, Roy P, Agrawal SK, Saxena AK (2010) Solvent free synthesis, anti-inflammatory and anticancer activity evaluation of tricyclic and tetracyclic benzimidazole derivatives. Bioorg Med Chem Lett 20: 2306.
12. Penning TD, Zhu GD, Gandhi VB, Gong J, Liu X, Shi Y, Klinghoffer V, Johnson EF, Donawho CK, Frost DJ, DiazBouska VB, Osterling DJ, Olson AM, Marsh KC, Luo Y, Giranda VL (2009) Discovery of the Poly(ADP-ribose) polymerase (PARP) inhibitor 2-[(R)-2-methylpyrrolidin-2-yl]-1H-benzimidazole-4-carboxamide (ABT-888) for the treatment of cancer. J Med Chem 52: 514.
13. Rashid M, Husain A, Mishra R (2012) Synthesis of benzimidazoles bearing oxadiazole nucleus as anticancer agents. Eur J Med Chem 54: 855-866.
14. Rashid M, Husain A, Mishra R, Karim S, Khan S, Ahmad M, Al-wabel N, Husain A, Ahmad A, Khan SA (2019) Design and synthesis of benzimidazoles containing substituted oxadiazole, thiadiazole and triazolothiadiazines as a source of new anticancer agents. Arab J Chem 12(8) 3202-3224.
15. Rashid M, Husain A, Shaharyar M, Sarafroz M (2014) Anticancer Activity of New Compounds Using Benzimidazole as a Scaffold. Anti-Cancer Agents in Med Chem 14: 1003-1018.

16. Husain A, Varshney MM, Rashid M, Mishra R, Akhter A (2011) Benzimidazole: A Valuable Insight in to the Recent Advances and Biological Activities. J Pharm Res 4: 413-419.
17. Lio SC, Johnson J, Chatterjee A, Ludwig JW, Millis D, Banie H, Sircar JC, Sinha A, Richards ML (2008) Disruption of golgi processing by 2-phenyl benzimidazole analogs blocks cell proliferation and slows tumor growth. Can Chemo Pharmaco 61: 1045.
18. Goker H, Kus C, Boykin DW, Yldz S, Altanlar N (2002) Synthesis of some new 2-substituted-phenyl-1H-benzimidazole-5-carbonitriles and their potent activity against Candida species. Bioorg Med Chem 10: 2589.
19. Kerimov I, Kilcigil GA, Eke BC, Altanlar N (2007) Synthesis, antifungal and antioxidant screening of some novel benzimidazole derivatives. J Enzyme Inhib Med 17: 696.
20. Sharma D, Narasimhan B, Kumar P, Judge V, Narang R, Clercq ED, Balzarini J (2009) Synthesis, antimicrobial and antiviral activity of substituted benzimidazoles. J Enzyme Inhib Med 24: 1161.
21. Kumar BVS, Vaidya SD, Kumar RV, Bhirud SB, Mane RB (2006) Biological activity evaluation of novel n-heterocyclic carbene precursors. Eur J Med Chem 41: 599.
22. Francisca P, Helgi JC, Jaime PV, Juan CP, Sergio RM, Guadalupe PH, Nayeli LB, Alicia HC, Rafael C, Francisco HL (2009) Synthesis and in-vitro cysticidal activity of new benzimidazole derivatives. Eur J Med Chem 44: 1794.
23. Padmavathi V, Reddy SG, Padmaja A, Kondaiah P, Shazia A (2009) Synthesis, antimicrobial and cytotoxic activities of 1,3,4-oxadiazoles, 1,3,4-thiadiazoles and 1,2,4-triazoles. Eur J Med Chem 44: 2106.
24. El-Sayed NS, El-Bendary ER, El-Ashry SM, El-Kerdawy MM (2011) Synthesis and antitumor activity of new sulfonamide derivatives of thiadiazolo[3,2-a]pyrimidines. Eur J Med Chem 46: 3714.
25. Formagio ASN, Tonin LTD, Foglio MA, Madjarof C, Carvalho JE, Costa WFD, Cardoso FP, Sarragiotto MH (2008) Synthesis of pyrrolo [2, 1-c] [1, 4] benzodiazepines. Bioorg Med Chem 16: 9660.
26. Matysiak J (2007) Evaluation of electronic, lipophilic and membrane affinity effects on antiproliferative activity of 5-substituted-2-(2,4-dihydroxyphenyl)-1,3,4-thiadiazoles against various human cancer cells. Eur J Med Chem 42: 940.
27. Lissitchkov T, Arnaudov G, Peytchev D, Merkle KJ (2006) Phase-I/II study to evaluate dose limiting toxicity, maximum tolerated dose, and tolerability of bendamustine HCl in pre-treated patients with B-chronic lymphocytic leukaemia (Binet stages B and C) requiring therapy. Canc Res Clin Onco 132: 99.
28. Naz S, Zahoor M, Umar MN, Alghamdi S, Sahibzada MUK, UlBari W.(2020)Synthesis, characterization, and pharmacological evaluation of thiourea derivative. Open Chem.18(1):764–77. doi: 10.1515/chem-2020-0139.
29. Goffin E, Lamoral-Theys D, Tajeddine N, de Tullio P, Mondin L, Lefranc F, et al. (2012) N-Aryl-N′-(chroman-4-yl)ureas and thioureas display in vitro anticancer activity and selectivity on apoptosis- resistant glioblastoma cells: screening, synthesis of simplified derivatives, and structure-activity relationship analysis. Eur J Med Chem. 54:834–44. doi: 10.1016/j.ejmech.2012.06.050.

30. Vega-Pérez JM, Periñán I, Argandoña M, Vega-Holm M,Palo-Nieto C, Burgos-Morón E, et al. (2012) Isoprenyl-thiourea and urea derivatives as new farnesyl diphosphate analogues: synthesis and in vitro antimicrobial and cytotoxic activities.Eur J Med Chem. 58:591–612. doi: 10.1016/j.ejmech.2012.10.042.
31. Ronchetti R, Moroni G, Carotti A, Gioiello A, Camaioni E. .(2021) Recent advances in urea- and thiourea-containing compounds: focus on innovative approaches in medicinal chemistry and organic synthesis. RSC Med Chem. 12(7):1046–64. doi: 10.1039/d1md00058f.
32. Madabhushi S, Mallu KKR, Vangipuram VS, Kurva S,Poornachandra Y, Ganesh Kumar C. (2014) Synthesis of novel benzimidazole functionalized chiral thioureas and evaluation of their antibacterial and anticancer activitiesBioorg Med Chem Lett.24(20):4822–5. doi: 10.1016/j.bmcl.2014.08.064.
33. Wang W, Kong D, Cheng H, Tan L, Zhang Z, Zhuang X, et al. (2014) New benzimidazole-2-urea derivates as tubulin inhibitors. Bioorg Med Chem Lett. 24(17):4250–3. doi: 10.1016/j.bmcl.2014.07.035.
34. Tahlan S, Kumar S, Kakkar S, Narasimhan B. .(2019) Benzimidazole scaffolds as promising antiproliferative agents: a reviewBMC Chem. 13(3):1–16. doi: 10.1186/s13065-019-0579-6.
35. Lipinski CA, Lombardo F, Dominy BW, Feeney PJ (1997) Experimental and computational approaches to estimate solubility and permeability in drug discovery and development settings. Adv Drug Deliver Rev 23: 4-25.
36. Ertl P, Rohde B, Selzer P (2000) Fast calculation of molecular polar surface area as a sum of fragment-based contributions and its application to the prediction of drug transport properties. J Med Chem 43: 3714-3717.
37. Molinspiration software (www.molinspiration.com/cgi-bin/properties).
38. Teague SJ, Davis AM, Leeson PD, Oprea T, Angew (1999) The Design of Lead like Combinatorial Libraries. Chem Int Ed 38: 3743.
39. Ghose AK, Viswanadhan VN, Wendoloski JJ (1999) A knowledge-based approach in designing combinatorial or medicinal chemistry libraries for drug discovery; A qualitative and quantitative characterization of known drug databases. J Comb Chem 1: 55.
40. Oprea TI (2000) Property distribution of drug-related chemical databases. J Comp Aided Mol Des 14: 251.
41. Kulkarni A, Han Y, Hopfinger AJJ (2002) Predicting Caco-2 cell permeation coefficients of organic molecules using membrane-interaction QSAR analysis, Chem. Inf Comput Sci 42: 331.
42. Veber DF, Johnson SR, Cheng HY, Smith BR, Ward KW, Kopple KD (2002) Molecular properties that influence the oral bioavailability of drug candidates. J Med Chem 45: 2615-2623.
43. Bhutani R, Pathak DP, Kapoor G, Husain A, Iqbal MA (2019) Novel hybrids of benzothiazole-1,3,4-oxadiazole-4-thiazolidinone: Synthesis, in-silico ADME study, molecular docking and in-vivo anti-diabetic assessment. Bioorg Chem 83: 6-19.
44. Faizia M, Jahania R, Ebadib SA, Tabatabaic SA, Rezaeec E, Lotfalieic M, Aminid M, Almasirad A (2017) Novel 4-thiazolidinone derivatives as agonists of benzodiazepine receptors: design, synthesis and pharmacological evaluation. EXCLI J 16: 52-62.
45. Kapoor G, Pathak DP, Bhutani R, Husain A, Jain S, Iqbal MA (2019) Synthesis, ADME, docking studies and in-vivo anti-hyperglycaemic potential

estimation of novel Schiff base derivatives from octadec-9-enoic acid. Bioorg Chem 84: 478-492.
46. Asif M, Acharya M, Lakshmayya Singh A (2015) In-silico physicochemical bioactivities and toxicities prediction of 3-chloro-6-arylpyridazines and 6-aryl-4,5-dihydropyridazine-3(2H)-thiones having antitubercular activity. RGUHS J Pharm Sci 5: 81-87.
47. Namachivayam B, Raj JS, Kandakatla N (2014) 2D, 3D-QSAR, docking and optimization of 5-substituted-1H-Indazole as inhibitors of GSK3β. Int J Pharm Pharm Sci 6: 1-8
48. Kulkarni A, Han Y, Hopfinger AJ (2002) PredictingCaco-2 cell permeation coefficients of organic molecules using membrane-interaction QSAR analysis, J. Chem. Inf. Comput. Sci. 42:331.
49. Hassan M, Ashraf Z, Abbas Q, Raza H (2018) Exploration of novel human tyrosinase inhibitors by molecular modeling, docking and simulation studies. Interdisciplinary Sci 3: 234.
50. Bhat AR, (2018) Petra, Osiris and Molinspiration: A computational bioinformatic platform for experimental in-vitro antibacterial activity of annulated uracil derivatives. Iranian Chemical Commun 7: 234.
51. Jamuna S, Rathinavel AK, Sadullah S, Sadullah M, Devaraj S (2018) In-silico approach to study the metabolism and biological activities of oligomeric proanthocyanidin complexes. Indian J Pharmacol 50: 242-250.
52. Joshi A, Kumar R, Sharma A (2018) Molecular docking studies, bioactivity score prediction, drug likeness analysis of gsk-3 β inhibitors: a target protein involved in alzheimer's disease. Biosci Biotech Res Asia 15:562-573.
53. Kumar SA, lakshmi NR, Priya SB, latha, BH, Megalai PM (2018) In-silico design, docking, and synthesis of 3-hydroxy-3-methylglutaryl-coenzyme A reductase inhibitors.Drug Inven. Today 10 (12): 2568-2581.
54. Molecular property explorer, OSIRIS properties [internet], 2014 [cited 2014 Nov 26], Available from http://www.organic-chemistry.org/prog/peo/drugscore.
55. Thomas S (2001) Actelion's property explorer, Actelion's Pharmaceuticals Ltd., Gewer bestrasse, 16: 4123 Allschwil, Switzerland
56. Balakrishnan N, Raj JS, Kandakatla N (2015) In-silico studies on new indazole derivatives as Gsk-3β inhibitors. Int J Pharm Pharm Sci 77 295-299.
57. Rashid M (2020) Design, synthesis and ADMET prediction of bis-benzimidazole as anticanceragent. Bioorg. Chem. 96: 103576.
58. Jagadish PC, Soni N, Verma A (2013) Design, synthesis and in-vitro antioxidant activity of 1, 3, 5-trisubstituted-2-pyrazolines derivatives. J Chem 4: 1-7.
59. Proudfoot JR (2002) Drugs, leads and drug-likeness: an analysis of some recently launched drugs. Bioorg Med Chem Lett 12(12): 1647-50.
60. Parua S, Sikari R, Singha S, Chakraborty G, Mondal R, Paul ND (2018) Accessing Polysubstituted Quinazolines via Nickel Catalyzed Acceptorless Dehydrogenative Coupling. J Org Chem 83: 11154-11166.
61. Caterina MC, Perillo IA, Boiani L, Pezaroglo H, Cerecetto H, Gonzalez M, Salerno A (2008) Imidazolidines as new anti-trypanosoma cruzi agents: biological evaluation and structureactivity relationships. Bioorg Med Chem 16: 2226-2234.

62. He T, Shi R, Gong Y, Jiang G, Liu M, Qian S, Wang Z (2016) Base-Promoted Cascade Approach for the preparation of reduced knoevenagel adducts using hantzsch esters as reducing agent in water. synlett 27: 1864-1869.
63. Lee SK, Chang GS, Lee IH, Chung JE, Sung KY, No KT (2004) The PreADME: Pc-Based program for batch prediction of ADME properties. Euro QSAR 9.5-10, Istanbul, Turkey.
64. Albert LP (2001) Screening for human ADME/Tox drug properties in drug discovery. DDT 6: 357-366.
65. Lee SK, Lee IH, Kim HJ, Chang GS, Chung JE, No KT (2003) The PreADME Approach: web-based program for rapid prediction of physicochemical, drug absorption and drug-like properties. Euro QSAR 2002 designing drugs and crop protectants: processes, problems and solutions, black well publishing, Massachusetts, USA, 418-420.
66. Wido, A., Bajamal, A. H., Apriawan, T., Parenrengi, M. A., & Al Fauzi, A. (2022). Deep vein thrombosis prophylaxis use in traumatic brain injury patients in tropical climate. International Journal of Health & Medical Sciences, 5(1), 67-74. https://doi.org/10.21744/ijhms.v5n1.1840
67. Ames test (2012, May 12). In Wikipedia, the Free Encyclopedia. Retrieved 14:44, May 21, 2012, fromhttp://en.wikipedia.org/w/index.php?title=Ames_test&oldid=492194122.
68. Zhang L, Brett CM, Giacomini KM (1998) Hayes' principles and methods of toxicology. Ann Rev Pharma Tox 38: 431.
69. Pradhan S, Mondal S, Sinha C (2016) In search of Tuberculosis drug design: An in-silico approach to azoimidazolyl derivatives as antagonist for Cytochrome P450. J Indian Chem Soc 93: 1-18.
70. Suryasa, I. W., Rodríguez-Gámez, M., & Koldoris, T. (2021). Get vaccinated when it is your turn and follow the local guidelines. International Journal of Health Sciences, 5(3), x-xv. https://doi.org/10.53730/ijhs.v5n3.2938
71. Md. Sarfaraj H, Faizul A, Hanan AE, Ismail A, Jamal AM, Jamal MD, Hend I, Mohammed A, Muhammad A, Anzarul H (2020) Anti-inflammatory, analgesic and molecular docking studies of Lanostanoic acid 3-O-a-D-glycopyranoside isolated from Helichrysum stoechas. Arab J Chem 13: 9196–9206.
72. Martin, T., (2016) Toxicity estimation software tool (TEST), US Environmental Protection Agency, Washington DC.
73. Sripriya N, Ranjith KM, Ashwin KN, Bhuvaneswari S, Udaya PNK (2019) In silico evaluation of multispecies toxicity of natural compounds. Drug Chem Toxicol. 21: 1-7.